HHS Public Access

Author manuscript

J Physiol. Author manuscript; available in PMC 2021 January 09.

Published in final edited form as:

J Physiol. 2020 January ; 598(2): 403–413. doi:10.1113/JP278768.

Intracranial pressure modulates aqueous humor dynamics of the eye

Kayla R. Ficarrotta[1], **Christopher L. Passaglia**[1,2]

[1]Medical Engineering Department, University of South Florida, Tampa, FL 33620

[2]Ophthalmology Department, University of South Florida, Tampa, FL 33620

Abstract

While intraocular pressure (IOP) is a well-known risk factor for glaucoma, intracranial pressure (ICP) is attracting heightened interest because of its influence on optic nerve head biomechanics. Studies have shown that ICP can have marked impact on posterior eye health by modifying the translaminar pressure gradient across the optic nerve. There is also growing evidence that IOP and ICP may be interconnected, though the mechanism of their putative interaction is unknown. We sought to test the hypothesis that ICP modulates IOP by altering aqueous humor dynamics. The anterior chamber and lateral ventricle of anesthetized Brown-Norway rats were cannulated with fine-gauge needles connected to a programmable pump and saline reservoir, respectively. ICP was manipulated by varying reservoir height, and eye outflow facility (C) was determined from the pump flowrate required to hold IOP at different levels. C was 22 ± 4 nl/min/mmHg at resting ICP and 13 ± 3 nl/min/mmHg when ICP was raised 15 mmHg, a reduction of 41 ± 13% (n=18). The decrease in outflow facility was independent of blood pressure, reversible, scaled with ICP elevation, and correlated with increases in resting IOP. It was physiological in origin because C returned to baseline values after euthanasia and corneal application of tetrodotoxin though ICP remained elevated. These results indicate that a neural feedback mechanism driven by ICP regulates conventional outflow facility in rats. The mechanism may protect the eye from translaminar pressure swings and may offer a new target for glaucoma treatment.

Keywords

glaucoma; conventional outflow facility; intraocular pressure

Corresponding author: Dr. Christopher L. Passaglia, Department of Medical Engineering, University of South Florida, 4202 E Fowler Ave, Tampa, FL 33620. Phone: 813-974-7140, passaglia@usf.edu.

Author Contributions

Experiments were performed in the laboratory of C.L.P. at the University of South Florida. K.R.F. conducted experiments, analyzed data, and drafted manuscript. C.L.P. assisted with experiment design, data analysis and manuscript editing. The authors each approved the final version of this manuscript, affirm that no other individuals qualify for authorship, and agree to be accountable for aspects of the work.

Competing Interests

The authors have no conflicts to disclose.

INTRODUCTION

The causal chain of events that link elevated intraocular pressure (IOP) to the onset and progression of glaucoma is not fully understood. There is consensus that IOP-induced stress and strain on the optic nerve head injure retinal ganglion cell (RGC) axons as they exit the eye through the lamina cribosa, leading to disrupted axoplasmic flow, RGC death, and permanent vision loss (Downs et al., 2008; Weinreb et al., 2014; Stowell et al., 2017). Yet it is acknowledged that high IOP is not the sole cause of the disease (Killer & Pircher, 2018). Other pathophysiological factors must exist because glaucomatous damage can occur in people with normal IOP (Klein et al., 1992) and normal tension glaucoma patients account for 30-92% of glaucoma diagnoses depending on race and ethnicity (Cho & Kee, 2014). Moreover, many people have ocular hypertension by clinical standards and never present signs of optic nerve injury (Kass et al., 2002; Gordon et al., 2011).

Another factor that has been hypothesized to play a role in glaucoma is cerebrospinal fluid pressure (CSFP). CSF fills the ventricles of the brain and surrounds the central nervous system to form a continuous fluid-filled compartment. The fluid applies pressure on the optic nerve head that can cause papilledema and nerve degeneration if too high (Hedges, 1975; Nusbaum et al., 2015; Shen et al., 2018). According to the CSFP hypothesis (Berdahl & Allingham, 2010) the mechanical insult to RGC axons depends not just on IOP but on the translaminar pressure (TLP) across the lamina cribosa, which is determined by the difference between IOP and CSFP. Low CSFP could thereby have similar impact on the optic nerve as high IOP, which may explain normal tension glaucoma, while high CSFP might counteract effects of high IOP, which could explain ocular hypertension without glaucoma (Morgan et al., 2008; Berdahl et al., 2012). The hypothesis has not been validated clinically because CSFP is difficult to access within retrolaminar tissue of the human optic nerve. However, it is supported by lumbar CSFP and intracranial pressure (ICP) measurements in humans (Berdahl et al., 2008; Ren et al., 2010; Ren et al., 2011; Siaudvytyte et al., 2014), which animal studies found to be nearly equivalent to retrolaminar tissue pressure for CSFP above ~2 mmHg (Morgan et al., 1995; Morgan et al., 1998). Animal studies have also shown that chronically lowering CSFP with a lumbar shunt can induce glaucomatous pathologies, including enlarged cup-to-disc ratio, reduced neuroretinal rim area, and retinal nerve fiber layer thinning (Yang et al., 2014).

Given the potential significance of TLP to glaucoma pathophysiology, it is important to know whether IOP and ICP are independently controlled variables in the body. Clinical evidence of a relationship is mixed. Several groups have reported that IOP is positively correlated with ICP in children and adults with varying degrees of hydrocephalus and no known history of glaucoma (Lashutka et al., 2004; Sajjadi et al., 2006; Spentzas et al., 2010; Li et al., 2012). The finding was subsequently verified by two large population-based studies (Jonas et al., 2013; Wang et al., 2014). However, a number of groups have not observed a significant association between IOP and ICP clinically (Han et al., 2008; Czarnik et al., 2009; Kirk et al., 2011). The discord may reflect differences in methodology, data analysis, and patient pools since one group noticed a strong correlation within subjects but not across subjects (Sheeran et al., 2000). Animal studies support a relationship. IOP was found to increase within minutes of expanding a subcranial balloon in monkeys (Lehman et al., 1972)

and to covary with ICP after hypothalamic stimulation in rats (Samuels et al., 2012) and carbon dioxide inhalation in horses (Cullen et al., 1990). No study to date has provided a physiological explanation for these clinical and experimental observations. The objective of this research was to test the hypothesis that IOP and ICP are physiologically connected and elucidate the mechanism underlying their putative relationship.

METHODS

Ethical approval

All experiments were conducted according to a protocol approved by the Institutional Animal Care and Use Committee at the University of South Florida in accordance with NIH guidelines and the ARVO statement for the use of animals in ophthalmic and vision research. Animals were obtained from a commercial supplier (Envigo, Indianapolis, IN) and euthanized at the end of experiments with Somnasol (Henry Schein, Melville, NY) given to effect. The authors confirm that the research conducted in this manuscript complies with the policies and regulations of the Journal of Physiology (Grundy, 2015).

Experimental setup

Male retired-breeder Brown-Norway rats (300-400 g) were housed under a 12hr:12hr light-dark cycle (6AM:6PM) with ad libitum access to food and water. On the day of experimentation animals were anesthetized via an intraperitoneal injection of ketamine hydrochloride (75 mg/kg) and xylazine (7.5 mg/kg), supplemented as needed. Anesthesia was maintained by IV delivery of ketamine (30 mg/kg/hr) through a catheter inserted in the femoral vein. Body temperature, heart rate, and mean arterial pressure (MAP) were monitored and kept in a physiologically normal range by adjusting the anesthetic infusion rate as needed. Body temperature was recorded with a rectal thermometer and controlled with a heating pad, heart rate was recorded with ECG electrodes, and MAP was recorded with a pressure sensor connected to a saline-filled catheter (MicroRenathane®, Braintree Scientific Inc., Braintree, MA; length: 30 cm, lumen: 0.4 mm) inserted in the femoral artery. The animal was then positioned in a stereotaxic instrument, an incision was made in the scalp, and a 25G needle was advanced into the lateral ventricles through a 0.5-mm hole drilled in the skull 1-mm caudal and 1.5-mm lateral to Bregma (Paxinos & Watson, 1998). The needle was connected via a 3-way stopcock and polyethylene tubing (length: 45 cm, lumen: 0.4 mm) to a pressure sensor and a reservoir of physiological saline mixed with 1% green tissue marking dye (Davidson Marking System, Middleton, WI). After ventricle cannulation, indicated by a jump in pressure reading, the needle was fixed in place and the hole was sealed with dental cement (A-M Systems, Sequim, WA). Successful cannulation was verified by stabilization of ICP at >4 mmHg and post-experiment assessment of dye location. Ventricle cannulation was periodically checked by briefly closing the saline reservoir to the ICP sensor. Pupils of both eyes were dilated with 1% cyclopentolate hydrochloride drops to normalize pupil size and block pupillary changes. The anterior chamber of one eye was cannulated with a 33G needle connected via a 3-way stopcock and tubing (length: 45 cm, lumen: 0.4 mm) to a pressor sensor and a programmable syringe pump (NE-1000, New Era Pump Systems, Farmingdale, NY) filled with artificial aqueous humor (Ficarrotta et al., 2018). Corneas were kept moist by covering with clear contact

lenses (OcuScience®, Henderson, NV) and instilling every 10-15 minutes with saline drops. The cannula site was periodically checked to verify that there was no needle displacement, internal tissue damage, or visible fluid leakage.

Figure 1A depicts the experimental setup. Each pressure sensor (Model 26PC, Honeywell, Morristown, NJ) was calibrated against a mercury manometer prior to data collection. The calibration procedure has been described and the hydrodynamic properties of the eye perfusion system (e.g. needle resistance, tubing compliance) have been reported and were found to have negligible influence on outflow measurements (Ficarrotta et al., 2018). Pressure sensor outputs were amplified, low-pass filtered at 1 Hz, and digitized at 2 Hz by a custom LabView (National Instruments, Austin, TX) computer program. Data collection began when ICP and IOP settled at values that fluctuated <1 mmHg over 15 minutes. These values were defined as the resting ICP and IOP.

Data collection and analysis

The conventional outflow facility (C), or hydraulic conductance, of the eye was measured using a modified constant-pressure perfusion technique (Ficarrotta et al., 2018); in which, a control algorithm switched the pump on and off to maintain IOP within 2 mmHg of a user-specified level. Net outflow (F) was calculated for different IOP set points as the product of pump duty cycle (D) and pump flow rate (Fp). Fp was fixed at 1.5 μL/min as IOP measurement error of the perfusion system is negligible (<1 mmHg) at this low flow rate (Bello et al., 2017). D was measured from the times required to raise IOP by 2 mmHg (T_1: pump on) and for IOP to then fall by 2 mmHg (T_2: pump off). That is, $D = T_1/(T_1 + T_2)$. F is thus zero at resting IOP since there is no outflow from the pump. F data were averaged over 4-6 pump cycles for each IOP set point and linearly regressed against IOP to estimate C. In every experiment, outflow facility was measured at resting ICP and at ICP set 15 mmHg above the resting level. ICP was manipulated by varying reservoir height, and data were collected >30 minutes after height changes when ICP had stabilized at the target level. In some experiments, outflow facility was also measured for 5-mmHg step increments in ICP, after topical application of tetrodotoxin (TTX, 1 μg/μl in saline), or after animal euthanasia. Statistical significance was assessed for paired and unpaired datasets using Student t-tests and for multifactorial datasets using ANOVA and Tukey multiple comparison tests at an alpha level of 0.05 using SigmaPlot software (Systat Inc., San Jose, CA). Intra-experiment results are expressed as 95% confidence intervals in brackets and inter-experiment results as mean ± standard deviation.

Histological processing

After animal euthanasia the dye-perfused brain was excised and submerged in 10% neutral buffered formalin for 24-48 hours. Fixed brains were embedded in paraffin, sliced in 4-μm coronal sections, and mounted on gelatin-coated slides. Tissue sections were stained with hematoxylin and eosin, viewed under light microscopy, and digitally photographed.

RESULTS

Cerebral ventricle cannulation was validated by histological examination of the dye-perfused brain. Figure 1B shows clumps of dye molecules in multiple widespread locations of the lateral ventricles but not in surrounding brain tissue, indicating that the ventricles were successfully cannulated in this experiment. The result was the same for every brain examined (n = 8). The absence of tissue staining was not an artifact of histological processing or tracer diffusion away from the cannulation site because dye was injected into brain tissue of control animals and the targeted area was loaded with tracer.

Figure 2A shows representative IOP, ICP, and MAP data collected from an anesthetized rat. Resting IOP and ICP levels averaged 14.5 ± 2.0 and 5.8 ± 1.9 mmHg, respectively, across all animals (n = 18), which translated to a resting TLP of 8.8 ± 2.9 mmHg. After baseline pressures were established, eye outflow facility was estimated by measuring the pump duty cycle required to hold IOP at various levels. It can be seen that sustained and cyclic IOP changes driven by the pump had no discernible effect on the resting ICP of this animal, nor the population of animals (ΔICP = 1.1 ± 1.7 mmHg, p = 0.07). IOP elevation did not alter MAP in those examined either (n = 7, ΔMAP = −0.3 ± 0.7 mmHg, p = 0.27). ICP was then raised 15 mmHg above its resting level, and outflow facility measurements were repeated with IOP held at the same levels by the pump. ICP elevation led to a small increase in the resting IOP of this animal as well as the population of animals (Table 1, ΔIOP = 3.0 ± 1.9 mmHg, p < 0.01). It had no discernible effect on MAP (ΔMAP = 0.5 ± 0.8 mmHg, p = 0.16). Figure 2B compares IOP records for one of the holding levels. It can be seen that ICP elevation also caused the duration of pump cycles to lengthen. Since pump rate is fixed, the longer cycle time implies a change in aqueous humor dynamics of the eye.

ICP manipulation had marked impact on eye outflow facility. Figure 3A shows pressure-flow data of a rat eye at resting and elevated ICP. The data are approximately linear over the range tested, and the decrease in slope indicates that conventional outflow facility was reduced at high ICP. Figure 3B summarizes outflow facility measurements across animals for an ICP elevation of 15 mmHg (n = 18). C was 22 ± 4 nl/min/mmHg at resting ICP, which is indistinguishable (p = 0.68) from reported values in rats not subjected to cerebral ventricle cannulation (Ficarrotta et al., 2018). C was 13 ± 3 nl/min/mmHg at high ICP, a reduction of 41.0 ± 13.4% (p < 0.01). The decrease in C was correlated across animals with the small increase in IOP that accompanied ICP elevation (R^2 = 0.54). It should be noted that measured values of C (Table 1) could differ for other IOP ranges if the pressure-flow relation of rat eyes is nonlinear, as reported for enucleated mouse eyes (Madekurozwa et al., 2017). In some experiments ICP was subsequently lowered back to the resting level to check for reproducibility. Figure 3C shows pressure-flow data of a rat eye before, during, and after ICP elevation. It can be seen that the slope returned to near-baseline when resting ICP was restored. Figure 3D summarizes outflow facility measurements for this subset of animals (n = 4). No difference in C was noted pre- and post-ICP elevation (p = 0.90) and both were significantly greater than C during ICP elevation (p < 0.01), demonstrating that the change in outflow facility was reversible. The effect of ICP on aqueous humor dynamics was also graded in magnitude. Figure 3E shows pressure-flow data of a rat eye in which several ICP levels were tested in a subset of animals (n = 4). It can be seen that C decreased

systematically as ICP was raised in steps of 5 mmHg. Figure 3F indicates that the relationship was approximately linear over the range tested, with an average slope of −0.7 nl/min/mmHg IOP per mmHg ICP across the group, and that resting IOP shifted progressively higher with ICP elevation, with an average slope of 0.3 mmHg per mmHg ICP due presumably to the declining outflow facility.

Measurements were repeated on dead eyes as a control. Figure 4 shows pressure-flow data of a rat eye at resting ICP, elevated ICP, and elevated ICP after animal euthanasia. The dead-eye data are shifted leftward since there is no aqueous production to maintain a resting IOP. It can be seen that C decreased after ICP elevation but returned to near-baseline after euthanasia although ICP remained high. C at elevated ICP was 19 ± 4 nl/min/mmHg across experiments on dead eyes (n = 10). This is greater than C at elevated ICP (13 ± 3 nl/min/mmHg, $p < 0.01$) and not different from C at resting ICP (22 ± 3 nl/min/mmHg, $p = 0.07$) when those eyes were alive. The effect of ICP on conventional outflow facility thus appears physiological in origin.

To determine whether neural signaling pathways might be involved, TTX was applied to the cornea of the eye. Figure 5A shows pressure-flow data of a rat eye at resting ICP, elevated ICP, and elevated ICP after application of the voltage-gated sodium-channel blocker. TTX partially or completely eliminated ICP-dependent changes in outflow facility for every animal tested (n = 4). Figure 5B summarizes the results of TTX experiments. C at resting ICP and elevated ICP was 23 ± 2 and 13 ± 3 nl/min/mmHg, respectively ($p = 0.01$). After drug application, C at elevated ICP was 21 ± 6 nl/min/mmHg, which is larger than the pre-TTX level ($p = 0.03$) and not different from the resting ICP level ($p = 0.63$). TTX also eliminated the small change in IOP associated with ICP elevation (pre-TTX: ΔIOP = 2.5 ± 2.0 mmHg, post-TTX: ΔIOP = −0.1 ± 1.2 mmHg, $p = 0.03$). TTX was also applied to a separate group of animals that were not subjected to ICP elevation. Figures 5C and 5D show that TTX had no discernible effect on outflow facility at resting ICP. C before and after drug application was 25 ± 2 and 24 ± 3 nl/min/mm, respectively (n = 3, $p = 0.46$). IOP was unchanged as well (ΔIOP = −0.6 ± 1.1 mmHg, $p = 0.47$).

DISCUSSION

IOP regulation is a subject of significant scientific, clinical, and pharmaceutical interest. This study reports the discovery of a novel mechanism of IOP regulation that depends on ICP. Prior research hints at the existence of such a mechanism (Lehman et al., 1972; Lashutka et al., 2004; Sajjadi et al., 2006; Samuels et al., 2012), but the possibility had not been experimentally investigated until now. Aqueous humor dynamics were quantified while ICP was acutely varied in anesthetized rats, and it was discovered that IOP systematically increased and conventional outflow facility decreased with ICP elevation up to 15 mmHg above the resting level. The inverse effect on IOP and C may be understood from the Goldmann equation (Brubaker, 2004): $IOP = (F_{in} - F_{un})/C + EVP$, where F_{in} is fluid influx rate due to aqueous humor production, F_{un} is fluid efflux rate via unconventional (non-trabecular) outflow pathways, and EVP is episcleral venous pressure. The equation indicates that a reduction in C would lead to a rise in IOP if other parameters remain constant.

The Goldmann equation offers quantitative predictions about the effect of ICP on aqueous humor dynamics. Assuming ICP only modulates outflow facility the equation can be rewritten for the purpose of this study as: $\Delta IOP = -\frac{\Delta C}{\Delta C + C}(IOP - EVP)$, where ΔIOP and ΔC are the respective change in IOP and C from their resting level. EVP data were not collected but measured values of IOP, ΔIOP, and ΔC (Table 1) would imply that it averaged 9.9 mmHg across animals. This fits reported values in mice and rabbits (Aihara et al., 2003a, b; Lavery & Kiel, 2013). However, it is above the 7.8 ± 1.3 mmHg range of the one study that has measured EVP in rats (Strohmaier et al., 2013). That study employed Sprague-Dawley rats so the discrepancy could perhaps reflect species differences in EVP, which have been noted in mice (Millar et al., 2015). A lower-than-predicted EVP level would imply larger-than-observed IOP changes, meaning that ICP elevation may have increased EVP in addition to outflow facility.

Several other pathways can be envisioned by which ICP could influence IOP. The simplest is biophysical. ICP elevation pushes CSF toward the eye, pressing the optic nerve head inward. A compression of intraocular volume would result in higher IOP based on Laplace's Law if wall tension stays constant. This explanation is unlikely, though, given the tiny tissue displacements involved (Zhao et al., 2015). Another is that ICP could modify intraocular fluid dynamics since IOP must scale with ocular volume if corneoscleral elastance is constant. Ocular volume fluctuations are driven by aqueous humor and blood. Aqueous volume depends on production rate and outflow facility. Production is driven primarily by active transport processes in the ciliary body. These processes require blood flow but are fairly independent of perfusion pressure based on studies of arterially-perfused bovine eyes (Wilson et al., 1993). This suggests that effects of ICP on IOP are not mediated by pressure-driven changes in aqueous production, which would agree with our finding that MAP was unaltered. Aqueous production is also modulated by a circadian clock that controls IOP (Liu & Shieh, 1995). The clock has circuit components in the suprachiasmatic nucleus (SCN) of the brain (Smith & Gregory, 1989; Liu & Shieh, 1995), and electrical and chemical stimulation of tissues surrounding the SCN has been shown to increase both ICP and IOP (Schmerl & Steinberg, 1948; Grimes et al., 1956; Samuels et al., 2012). ICP elevation could thus raise IOP by mechanically or physiologically activating cells along the circadian pathway. Blood volume, in turn, depends on retinal and ciliary artery flow and venous resistance. Intracranial hypertension has been reported to decrease ocular blood flow and increase blood pressure by constricting outflow vessels (Querfurth et al., 2002; Miller et al., 2009; Firsching et al., 2011). Since IOP correlates strongly with retinal artery and vein pressure (Attariwala et al., 1994; Westlake et al., 2001) it should change with ICP as well. Ocular blood flow is also regulated by autonomic neurons in the brainstem that innervate the choroid (Steinle et al., 2000; Strohmaier et al., 2013). ICP elevation could activate these cells directly or indirectly via nerve projections from the hypothalamus (Li et al., 2010) and other brain areas (Li et al., 2015). Another possibility is the ciliary nerve innervating the cornea, iris, and ciliary muscle. IOP increases have been reported after pupil dilation with mydriatics (Kim et al., 2012) and after electrical stimulation of the ciliary ganglion (Schmerl & Steinberg, 1949; Grimes et al., 1956). Pupil abnormalities have been noted in patients with intracranial hypertension as well (Marshall et al., 1983).

While the above mechanisms may have contributed to observed IOP increases, they do not explain ICP effects on conventional outflow facility. Ocular volume and EVP changes would shift pressure-flow data laterally but not alter their slope, and ciliary muscle movements were blocked during data collection with mydriatics. Our results indicate that neural feedback signals from the brain directly modulate outflow facility. The likely site of neuromodulation is the inner wall region of Schlemm's canal, which presents the main source of outflow resistance (Johnson, 2006). Moreover, the trabecular meshwork is innervated by parasympathetic and sympathetic nerve fibers that could influence the contractile state of active elements within the meshwork and alter the passage of aqueous into the canal (Ehinger, 1971; Nomura & Smelser, 1974; Ruskell, 1976; Overby et al., 2014). Flow through drainage vessels downstream of the canal may also be subjected to some degree of neuromodulation, as nerve terminals are found throughout the chamber angle and next to episcleral vasculature (Collins et al., 1956; Selbach et al., 2005).

Figure 6 summarizes our results in the form of a working model. It is postulated that there exists an ICP-driven neural feedback mechanism which acts to protect the optic nerve from damage by altering TLP. ICP elevation activates, by unknown means, neurons in the brain that send signals back to the eye via the ciliary nerve or other autonomic nerve projection (McDougal & Gamlin, 2015). The efferent signals trigger an increase in resistance of aqueous outflow pathways, raising IOP and lowering TLP towards baseline level. One might expect a complete restoration of baseline TLP based on the CSFP hypothesis (Berdahl & Allingham, 2010), but this was not observed and might not be necessary for a protective effect. Computational models indicate that IOP has much larger influence on optic nerve head biomechanics than ICP and that TLP alone is insufficient to capture their complex interaction with material properties (Hua et al., 2018; Tong et al., 2019). The feedback mechanism does not operate in reverse since ICP was unaffected by IOP elevation, and it appears inactive under normal operating conditions since TTX application had no effect on outflow facility at resting ICP. Of importance for further study are feedback dynamics and short- and long-term physiological effectiveness. Efferent modulation of C and IOP was revealed here via acute steps in ICP. Feedback response time was not investigated nor whether the mechanism adapts or fatigues to sustained activation, given that chronic ICP elevation was found to cause optic nerve degeneration in mice (Nusbaum et al., 2015; Shen et al., 2018). The discovery of a central regulator of aqueous humor dynamics in rats may offer a new target for glaucoma treatment.

Supplementary Material

Refer to Web version on PubMed Central for supplementary material.

Acknowledgments

Funding

The work was supported by NIH grant R01 EY027037 to C.L.P.

REFERENCES

Aihara M, Lindsey JD & Weinreb RN. (2003a). Aqueous humor dynamics in mice. Invest Ophthalmol Vis Sci 44, 5168–5173. [PubMed: 14638713]

Aihara M, Lindsey JD & Weinreb RN. (2003b). Episcleral venous pressure of mouse eye and effect of body position. Curr Eye Res 27, 355–362. [PubMed: 14704919]

Attariwala R, Giebs CP & Glucksberg MR. (1994). The influence of elevated intraocular pressure on vascular pressures in the cat retina. Invest Ophthalmol Vis Sci 35, 1019–1025. [PubMed: 8125712]

Bello SA, Malavade S, Passaglia CL. (2017). Development of a smart pump for monitoring and controlling intraocular pressure. Ann Biomed Eng 45, 990–1002. [PubMed: 27679446]

Berdahl JP & Allingham RR. (2010). Intracranial pressure and glaucoma. Curr Opin Ophthalmol 21, 106–111. [PubMed: 20040876]

Berdahl JP, Allingham RR & Johnson DH. (2008). Cerebrospinal fluid pressure is decreased in primary open-angle glaucoma. Ophthalmology 115, 763–768. [PubMed: 18452762]

Berdahl JP, Yu DY & Morgan WH. (2012). The translaminar pressure gradient in sustained zero gravity, idiopathic intracranial hypertension, and glaucoma. Med Hypotheses 79, 719–724. [PubMed: 22981592]

Brubaker RF. (2004). Goldmann's equation and clinical measures of aqueous dynamics. Exp Eye Res 78, 633–637. [PubMed: 15106943]

Cho HK & Kee C. (2014). Population-based glaucoma prevalence studies in Asians. Surv Ophthalmol 59, 434–447. [PubMed: 24837853]

Collins EM, Holland MG & Von Sallmann L. (1956). A study of the innervation of the chamber angle. Am J Ophthalmol 42, 148–161. [PubMed: 13372663]

Cullen LK, Steffey EP, Bailey CS, Kortz G, da Silva Curiel J, Bellhorn RW, Woliner MJ, Elliott AR & Jarvis KA. (1990). Effect of high PaCO2 and time on cerebrospinal fluid and intraocular pressure in halothane-anesthetized horses. Am J Vet Res 51, 300–304. [PubMed: 2301844]

Czarnik T, Gawda R, Kolodziej W, Latka D, Sznajd-Weron K & Weron R. (2009). Associations between intracranial pressure, intraocular pressure and mean arterial pressure in patients with traumatic and non-traumatic brain injuries. Injury 40, 33–39. [PubMed: 19135194]

Downs JC, Roberts MD & Burgoyne CF. (2008). Mechanical environment of the optic nerve head in glaucoma. Optom Vis Sci 85, 425–435. [PubMed: 18521012]

Ehinger B (1971). A comparative study of the adrenergic nerves to the anterior eye segment of some primates. Z Zellforsch Mikrosk Anat 116, 157–177. [PubMed: 4996102]

Ficarrotta KR, Bello SA, Mohamed YH & Passaglia CL. (2018). Aqueous Humor Dynamics of the Brown-Norway Rat. Invest Ophthalmol Vis Sci 59, 2529–2537. [PubMed: 29847660]

Firsching R, Müller C, Pauli SU, Voellger B, Röhl FW & Behrens-Baumann W. (2011). Noninvasive assessment of intracranial pressure with venous ophthalmodynamometry. Clinical article. J Neurosurg 115, 371–374. [PubMed: 21529131]

Gordon MO, Gao F, Beiser JA, Miller JP & Kass MA. (2011). The 10-year incidence of glaucoma among patients with treated and untreated ocular hypertension. Arch Ophthalmol 129, 1630–1631. [PubMed: 22159688]

Grimes PA, Macri FJ, Von Sallmann L & Wanko T. (1956). Some mechanisms of centrally induced eye pressure responses. Am J Ophthalmol 42, 130–147. [PubMed: 13372662]

Grundy D (2015). Principles and standards for reportinganimal experiments in The Journal of Physiology and Experimental Physiology. J Physiol 593, 2547–2549. [PubMed: 26095019]

Han Y, McCulley TJ & Horton JC. (2008). No correlation between intraocular pressure and intracranial pressure. Ann Neurol 64, 221–224. [PubMed: 18570302]

Hedges TR. (1975). Papilledema: its recognition and relation to increased intracranial pressure. Surv Ophthalmol 19, 201–223. [PubMed: 1089322]

Hua Y, Voorhees AP & Sigal IA. (2018). Cerebrospinal fluid pressure: revisiting factors Influencing optic nerve head biomechanics. Invest Ophthalmol Vis Sci 59, 154–165. [PubMed: 29332130]

Johnson M (2006). What controls aqueous humour outflow resistance? Exp Eye Res 82, 545–557. [PubMed: 16386733]

Jonas JB, Nangia V, Wang N, Bhate K, Nangia P, Yang D, Xie X & Panda-Jonas S. (2013). Trans-lamina cribrosa pressure difference and open-angle glaucoma. The central India eye and medical study. PLoS One 8, e82284. [PubMed: 24324767]

Kass MA, Heuer DK, Higginbotham EJ, Johnson CA, Keltner JL, Miller JP, Parrish RK 2nd, Wilson MR & Gordon MO. (2002). The Ocular Hypertension Treatment Study: a randomized trial determines that topical ocular hypotensive medication delays or prevents the onset of primary open-angle glaucoma. Arch Ophthalmol 120, 701–713; discussion 829-730. [PubMed: 12049574]

Killer HE & Pircher A. (2018). Normal tension glaucoma: review of current understanding and mechanisms of the pathogenesis. Eye (Lond) 32, 924–930. [PubMed: 29456252]

Kim JM, Park KH, Han SY, Kim KS, Kim DM, Kim TW & Caprioli J. (2012). Changes in intraocular pressure after pharmacologic pupil dilation. BMC Ophthalmol 12, 53. [PubMed: 23017184]

Kirk T, Jones K, Miller S & Corbett J. (2011). Measurement of intraocular and intracranial pressure: is there a relationship? Ann Neurol 70, 323–326. [PubMed: 21710618]

Klein BE, Klein R, Sponsel WE, Franke T, Cantor LB, Martone J & Menage MJ. (1992). Prevalence of glaucoma. The Beaver Dam Eye Study. Ophthalmology 99, 1499–1504. [PubMed: 1454314]

Lashutka MK, Chandra A, Murray HN, Phillips GS & Hiestand BC. (2004). The relationship of intraocular pressure to intracranial pressure. Ann Emerg Med 43, 585–591. [PubMed: 15111918]

Lavery WJ & Kiel JW. (2013). Effects of head down tilt on episcleral venous pressure in a rabbit model. Exp Eye Res 111, 88–94. [PubMed: 23567205]

Lehman RA, Krupin T & Podos SM. (1972). Experimental effect of intracranial hypertension upon intraocular pressure. J Neurosurg 36, 60–66. [PubMed: 4621385]

Li C, Fitzgerald ME, Del Mar N, Cuthbertson-Coates S, LeDoux MS, Gong S, Ryan JP & Reiner A. (2015). The identification and neurochemical characterization of central neurons that target parasympathetic preganglionic neurons involved in the regulation of choroidal blood flow in the rat eye using pseudorabies virus, immunolabeling and conventional pathway tracing methods. Front Neuroanat 9, 65. [PubMed: 26082687]

Li C, Fitzgerald ME, Ledoux MS, Gong S, Ryan P, Del Mar N & Reiner A. (2010). Projections from the hypothalamic paraventricular nucleus and the nucleus of the solitary tract to prechoroidal neurons in the superior salivatory nucleus: Pathways controlling rodent choroidal blood flow. Brain Res 1358, 123–139. [PubMed: 20801105]

Li Z, Yang Y, Lu Y, Liu D, Xu E, Jia J, Yang D, Zhang X, Yang H, Ma D & Wang N. (2012). Intraocular pressure vs intracranial pressure in disease conditions: a prospective cohort study (Beijing iCOP study). BMC Neurol 12, 66. [PubMed: 22862817]

Liu JH & Shieh BE. (1995). Suprachiasmatic nucleus in the neural circuitry for the circadian elevation of intraocular pressure in rabbits. J Ocul Pharmacol Ther 11, 379–388. [PubMed: 8590270]

Madekurozwa M, Reina-Torres E, Overby DR & Sherwood JM. (2017). Direct measurement of pressure-independent aqueous humour flow using iPerfusion. Exp Eye Res 162, 129–138. [PubMed: 28720436]

Marshall LF, Barba D, Toole BM & Bowers SA. (1983). The oval pupil: clinical significance and relationship to intracranial hypertension. J Neurosurg 58, 566–568. [PubMed: 6827351]

McDougal DH & Gamlin PD. (2015). Autonomic control of the eye. Compr Physiol 5, 439–473. [PubMed: 25589275]

Millar JC, Phan TN, Pang IH & Clark AF. (2015). Strain and Age Effects on Aqueous Humor Dynamics in the Mouse. Invest Ophthalmol Vis Sci 56, 5764–5776. [PubMed: 26325415]

Miller MM, Chang T, Keating R, Crouch E & Sable C. (2009). Blood flow velocities are reduced in the optic nerve of children with elevated intracranial pressure. J Child Neurol 24, 30–35. [PubMed: 19168816]

Morgan WH, Yu DY, Alder VA, Cringle SJ, Cooper RL, House PH & Constable IJ. (1998). The correlation between cerebrospinal fluid pressure and retrolaminar tissue pressure. Invest Ophthalmol Vis Sci 39, 1419–1428. [PubMed: 9660490]

Morgan WH, Yu DY & Balaratnasingam C. (2008). The role of cerebrospinal fluid pressure in glaucoma pathophysiology: the dark side of the optic disc. J Glaucoma 17, 408–413. [PubMed: 18703953]

Morgan WH, Yu DY, Cooper RL, Alder VA, Cringle SJ & Constable IJ. (1995). The influence of cerebrospinal fluid pressure on the lamina cribrosa tissue pressure gradient. Invest Ophthalmol Vis Sci 36, 1163–1172. [PubMed: 7730025]

Nomura T & Smelser GK. (1974). The identification of adrenergic and cholinergic nerve endings in the trabecular meshwork. Invest Ophthalmol 13, 525–532. [PubMed: 4135124]

Nusbaum DM, Wu SM & Frankfort BJ. (2015). Elevated intracranial pressure causes optic nerve and retinal ganglion cell degeneration in mice. Exp Eye Res 136, 38–44. [PubMed: 25912998]

Overby DR, Bertrand J, Schicht M, Paulsen F, Stamer WD & Lütjen-Drecoll E. (2014). The structure of the trabecular meshwork, its connections to the ciliary muscle, and the effect of pilocarpine on outflow facility in mice. Invest Ophthalmol Vis Sci 55, 3727–3736. [PubMed: 24833737]

Paxinos G & Watson C. (1998). The rat brain in stereotaxic coordinates. Academic Press, San Diego, CA.

Querfurth HW, Lagrèze WD, Hedges TR & Heggerick PA. (2002). Flow velocity and pulsatility of the ocular circulation in chronic intracranial hypertension. Acta Neurol Scand 105, 431–440. [PubMed: 12027831]

Ren R, Jonas JB, Tian G, Zhen Y, Ma K, Li S, Wang H, Li B, Zhang X & Wang N. (2010). Cerebrospinal fluid pressure in glaucoma: a prospective study. Ophthalmology 117, 259–266. [PubMed: 19969367]

Ren R, Zhang X, Wang N, Li B, Tian G & Jonas JB. (2011). Cerebrospinal fluid pressure in ocular hypertension. Acta Ophthalmol 89, e142–148. [PubMed: 21348961]

Ruskell GL. (1976). The source of nerve fibres of the trabeculae and adjacent structures in monkey eyes. Exp Eye Res 23, 449–459. [PubMed: 824151]

Sajjadi SA, Harirchian MH, Sheikhbahaei N, Mohebbi MR, Malekmadani MH & Saberi H. (2006). The relation between intracranial and intraocular pressures: study of 50 patients. Ann Neurol 59, 867–870. [PubMed: 16634008]

Samuels BC, Hammes NM, Johnson PL, Shekhar A, McKinnon SJ & Allingham RR. (2012). Dorsomedial/Perifornical hypothalamic stimulation increases intraocular pressure, intracranial pressure, and the translaminar pressure gradient. Invest Ophthalmol Vis Sci 53, 7328–7335. [PubMed: 23033392]

Schmerl E & Steinberg B. (1948). The role of the diencephalon in regulating ocular tension. Am J Ophthalmol 31, 155–158. [PubMed: 18905670]

Schmerl E & Steinberg B. (1949). The role of ciliary and superior cervical ganglia in ocular tension. Am J Ophthalmol 32, 947–950. [PubMed: 18153960]

Selbach JM, Rohen JW, Steuhl KP & Lütjen-Drecoll E. (2005). Angioarchitecture and innervation of the primate anterior episclera. Curr Eye Res 30, 337–344. [PubMed: 16020264]

Sheeran P, Bland JM & Hall GM. (2000). Intraocular pressure changes and alterations in intracranial pressure. Lancet 355, 899. [PubMed: 10752710]

Shen G, Link S, Kumar S, Nusbaum DM, Tse DY, Fu Y, Wu SM & Frankfort BJ. (2018). Characterization of Retinal Ganglion Cell and Optic Nerve Phenotypes Caused by Sustained Intracranial Pressure Elevation in Mice. Sci Rep 8, 2856. [PubMed: 29434244]

Siaudvytyte L, Januleviciene I, Ragauskas A, Bartusis L, Meiliuniene I, Siesky B & Harris A. (2014). The difference in translaminar pressure gradient and neuroretinal rim area in glaucoma and healthy subjects. J Ophthalmol 2014, 937360. [PubMed: 24876948]

Smith SD & Gregory DS. (1989). A circadian rhythm of aqueous flow underlies the circadian rhythm of IOP in NZW rabbits. Invest Ophthalmol Vis Sci 30, 775–778. [PubMed: 2703321]

Spentzas T, Henricksen J, Patters AB & Chaum E. (2010). Correlation of intraocular pressure with intracranial pressure in children with severe head injuries. Pediatr Crit Care Med 11, 593–598. [PubMed: 20081553]

Steinle JJ, Krizsan-Agbas D & Smith PG. (2000). Regional regulation of choroidal blood flow by autonomic innervation in the rat. Am J Physiol Regul Integr Comp Physiol 279, R202–209. [PubMed: 10896883]

Stowell C, Burgoyne CF, Tamm ER, Ethier CR & Participants LIIoAaGN. (2017). Biomechanical aspects of axonal damage in glaucoma: A brief review. Exp Eye Res 157, 13–19. [PubMed: 28223180]

Strohmaier CA, Reitsamer HA & Kiel JW. (2013). Episcleral venous pressure and IOP responses to central electrical stimulation in the rat. Invest Ophthalmol Vis Sci 54, 6860–6866. [PubMed: 24065806]

Tong J, Ghate D, Kedar S & Gu L. (2019). Relative Contributions of Intracranial Pressure and Intraocular Pressure on Lamina Cribrosa Behavior. J Ophthalmol 2019, 3064949. [PubMed: 31007950]

Wang YX, Jonas JB, Wang N, You QS, Yang D, Xie XB & Xu L. (2014). Intraocular pressure and estimated cerebrospinal fluid pressure. The Beijing Eye Study 2011. PLoS One 9, e104267. [PubMed: 25105777]

Weinreb RN, Aung T & Medeiros FA. (2014). The Pathophysiology and Treatment of Glaucoma: A Review. JAMA 311, 1901–1911. [PubMed: 24825645]

Westlake WH, Morgan WH & Yu DY. (2001). A pilot study of in vivo venous pressures in the pig retinal circulation. Clin Exp Ophthalmol 29, 167–170. [PubMed: 11446461]

Wilson WS, Shahidullah M & Millar C. (1993). The bovine arterially-perfused eye: an in vitro method for the study of drug mechanisms on IOP, aqueous humour formation and uveal vasculature. Curr Eye Res 12, 609–620. [PubMed: 7693396]

Yang D, Fu J, Hou R, Liu K, Jonas JB, Wang H, Chen W, Li Z, Sang J, Zhang Z, Liu S, Cao Y, Xie X, Ren R, Lu Q, Weinreb RN & Wang N. (2014). Optic neuropathy induced by experimentally reduced cerebrospinal fluid pressure in monkeys. Invest Ophthalmol Vis Sci 55, 3067–3073. [PubMed: 24736050]

Zhao D, He Z, Vingrys AJ, Bui BV & Nguyen CT. (2015). The effect of intraocular and intracranial pressure on retinal structure and function in rats. Physiol Rep 3.

TRANSLATIONAL PERSPECTIVE

Elevated intraocular pressure (IOP) is a primary risk factor for glaucoma, an insidious disease that causes blindness by killing retinal ganglion cells. Lowering IOP is thereby a focus of current treatment methods. Another potential factor is intracranial pressure (ICP) since it also contributes to the mechanical forces experienced by ganglion cell axons as they exit the eye. Research in this manuscript sought to test the hypothesis that IOP and ICP are physiologically connected. The discovery that IOP is modulated by a neural feedback pathway that is driven by ICP could have translational significance by revealing that IOP fluctuations depend in part on signals sent from the brain to the eyes. This could lead to new avenues for glaucoma treatment, wherein central feedback pathways might be used to help control IOP and impede disease progression.

Key Points

- ICP elevation lowers conventional outflow facility (increases aqueous outflow resistance) of rat eyes
- The reduction in outflow facility correlates with an increase in IOP
- The effect of ICP elevation on outflow facility and IOP is blocked by tetrodotoxin.
- The results indicate that aqueous humor dynamics is modulated by ICP-driven neural feedback from the brain.
- This feedback mechanism may act to stabilize translaminar pressure across the optic nerve head and may provide a new avenue for glaucoma therapy.

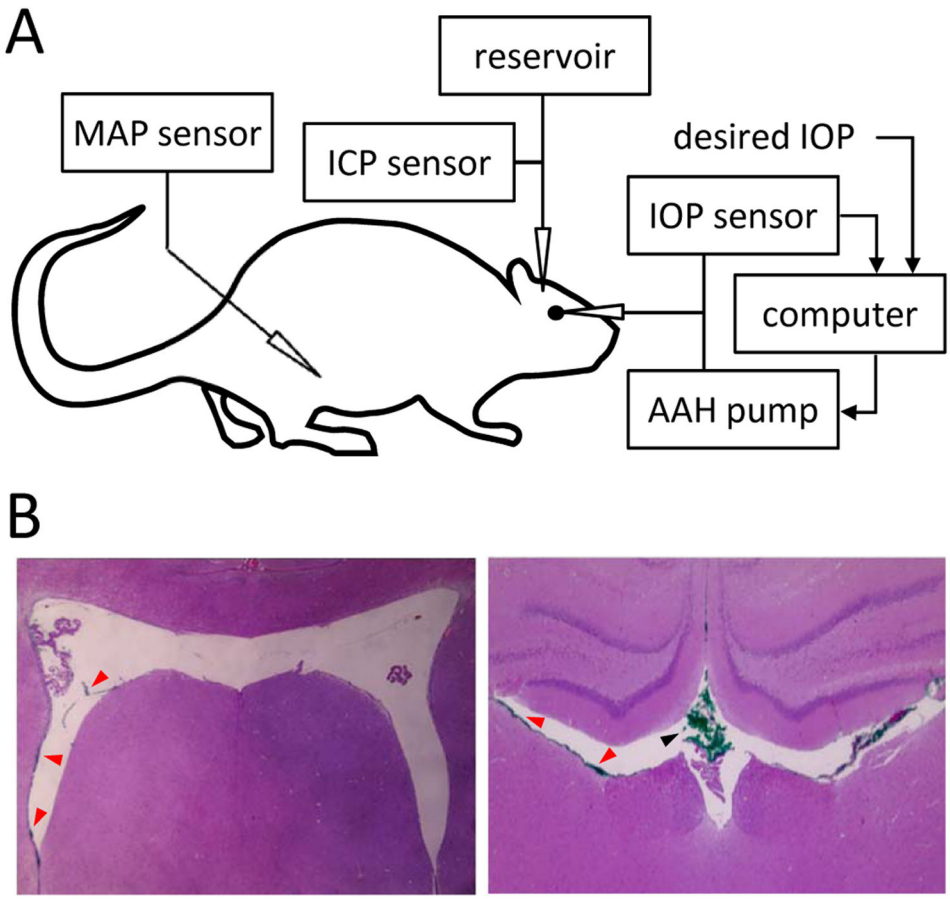

Figure 1.

Experimental setup. A, Intraocular pressure (IOP), intracranial pressure (ICP), and mean arterial pressure (MAP) were simultaneously recorded with separate pressure sensors via cannulas inserted in the anterior chamber of the eye, cerebral ventricles, and femoral artery, respectively. The IOP cannula was also connected to a pump that infused artificial aqueous humor (AAH) under computer control in order to measure conventional outflow facility. The ICP cannula was also connected to a variable-height reservoir of physiological saline in order to manipulate ICP level. B, Coronal tissue sections of a rat brain perfused with green tracer dye through the cannula. Sections are ~1 mm apart in the rostrocaudal direction. Red and black arrowheads indicate clumps of dye molecules in the lateral ventricles and dorsal third ventricle, respectively. No tracer was found in brain tissue in these or other sections.

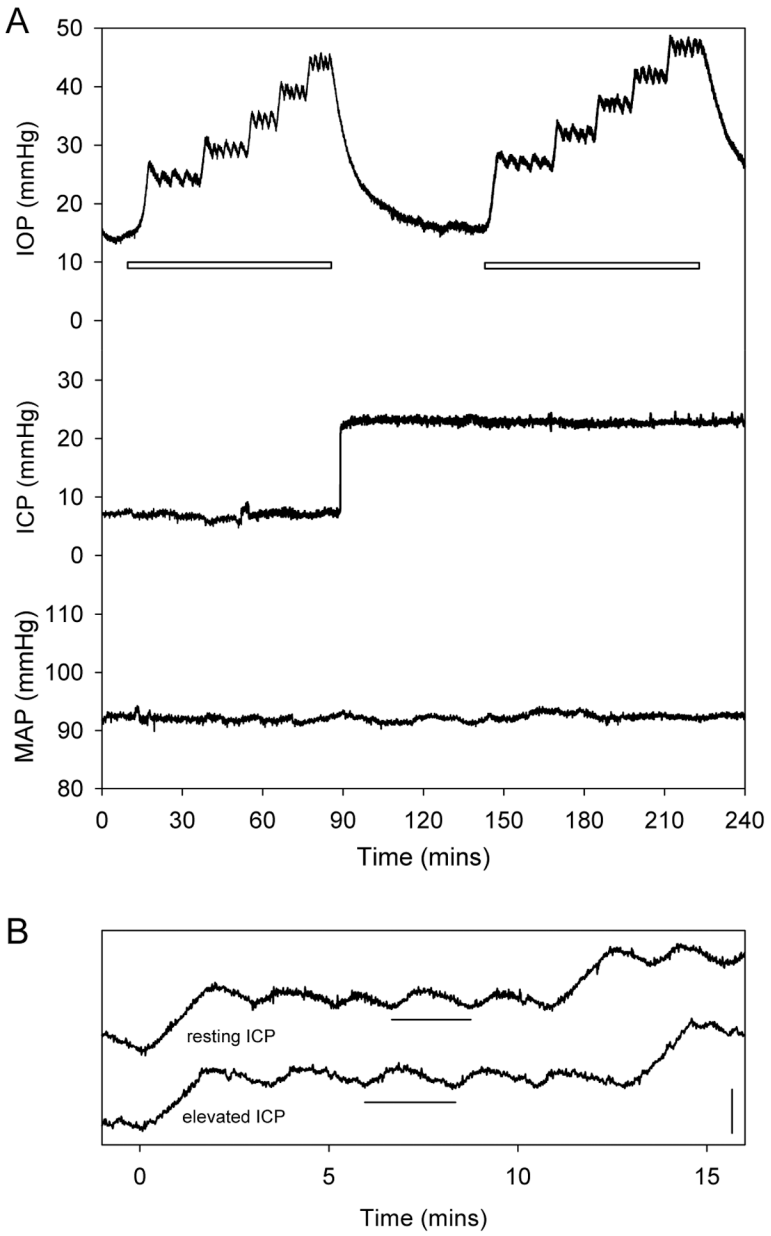

Figure 2.

IOP, ICP, and MAP records. A, Representative raw pressure data collected from an anesthetized rat before and after raising ICP by 15 mmHg. White bars indicate periods during which *C* was estimated by measuring the average pump duty cycle (i.e., flow rate) required to hold IOP at 10, 15, 20, 25, and 30 mmHg above its resting level. IOP, ICP, and MAP were 14.2 ± 0.4, 7.2 ± 0.3, and 92 ± 1 mmHg at rest, respectively, for this animal. B, IOP records for the +25 mmHg holding level in A shown on an expanded time scale. The records were displaced vertically and aligned to the same start time in order to facilitate visualization of the change in pump cycle duration (horizontal bars) before and after ICP elevation. Vertical bar is 5 mmHg in height.

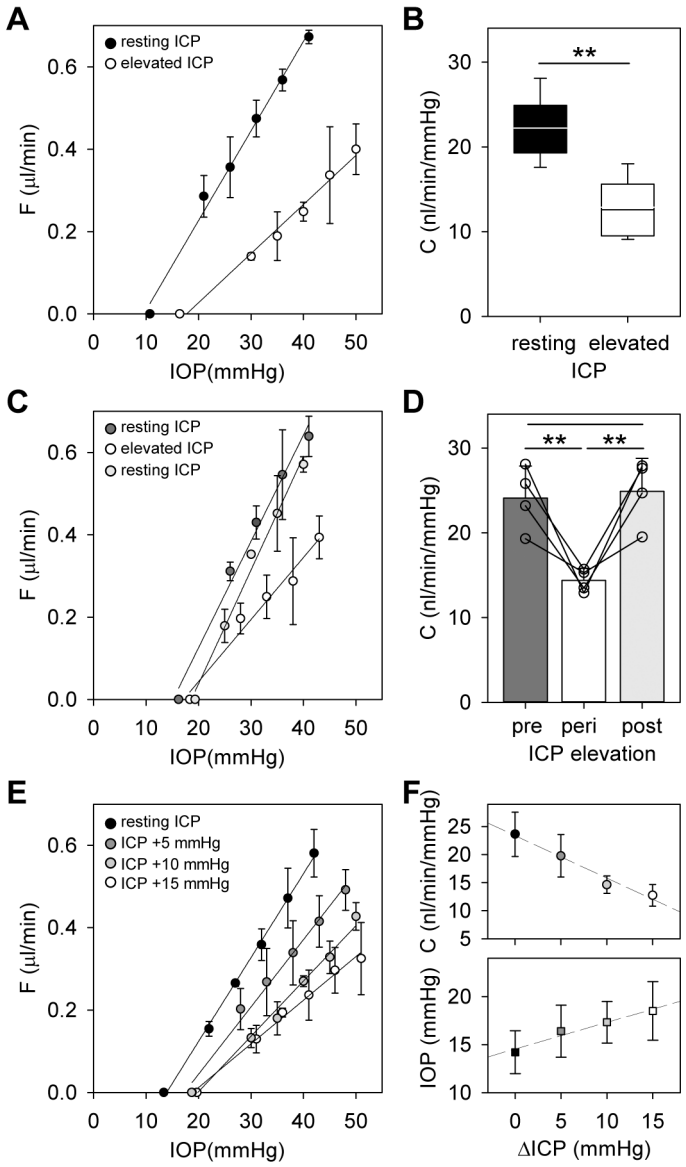

Figure 3.

Impact of ICP elevation on conventional outflow facility. A, Pressure-flow data of a rat eye at resting ICP of 4 mmHg (black symbols) and at ICP raised to 19 mmHg (white symbols). Data regression fits (lines) estimate *C* of 22 [20-24] and 12 [9-15] nl/min/mmHg, respectively. B, Summary of *C* data for all animals at resting ICP and 15 mmHg above resting ICP (n = 18). Box-and-whiskers plot median, 10th, 25th, 75th, and 90th percentiles. C, Pressure-flow data of a rat eye pre- (black symbols), peri- (white symbols), and post- (gray symbols) ICP elevation of 15mmHg. Data regression fits (lines) estimate *C* of 24 [20-28], 14 [10-17], and 25 [21-30] nl/min/mmHg, respectively. D, Average *C* for the subset of animals tested pre-, peri-, and post-ICP elevation (n = 4). E, Pressure-flow data of a rat eye at resting ICP (black symbols) and 5 (dark gray symbols), 10 (light gray symbols), and 15 mmHg (white symbols) above resting ICP. Data regression fits (lines) estimate *C* of 24 [20-27] at resting ICP and 19 [13-25], 16 [12-20], and 12 [9-15] nl/min/mmHg for

successive ICP increments. F, Average C (circles) and resting IOP (squares) for the subset of animals tested with multiple ICP levels (n = 4). Error bars give standard deviations, and asterisks indicate statistically significant differences ($p < 0.01$).

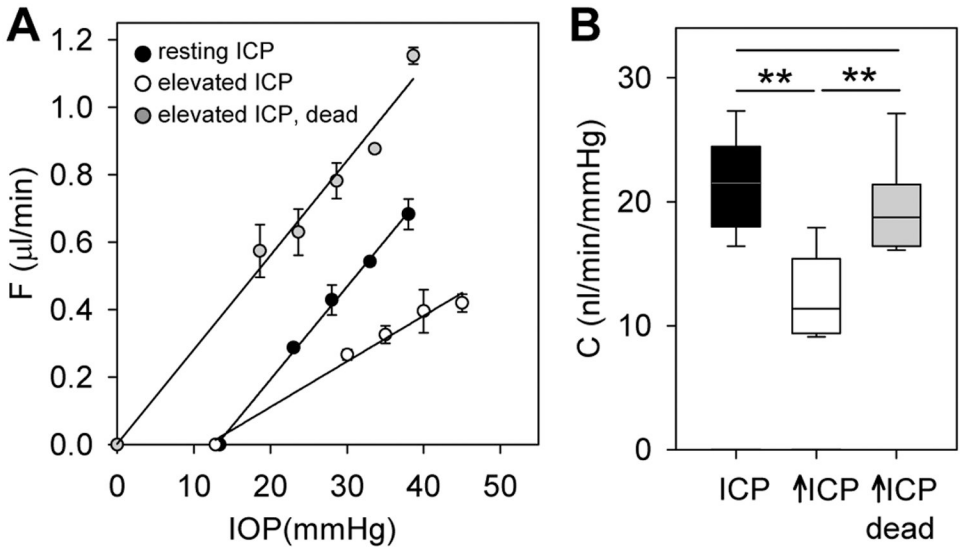

Figure 4.

ICP effect involves an active physiological process. A, Pressure-flow data of a rat eye at resting ICP (black symbols), 15 mmHg above resting ICP (white symbols), and 15 mmHg above resting ICP after animal euthanasia (gray symbols). Data regression fits (lines) estimate *C* of 27 [21-33], 13 [11-16], and 27 [22-32] nl/min/mmHg, respectively. B. Summary of *C* data for the subset of animals tested pre- and post-euthanasia (n = 10). Box-and-whiskers plot median, 10th, 25th, 75th, and 90th percentiles. Error bars give standard deviations, and asterisks indicate statistically significant differences ($p < 0.001$).

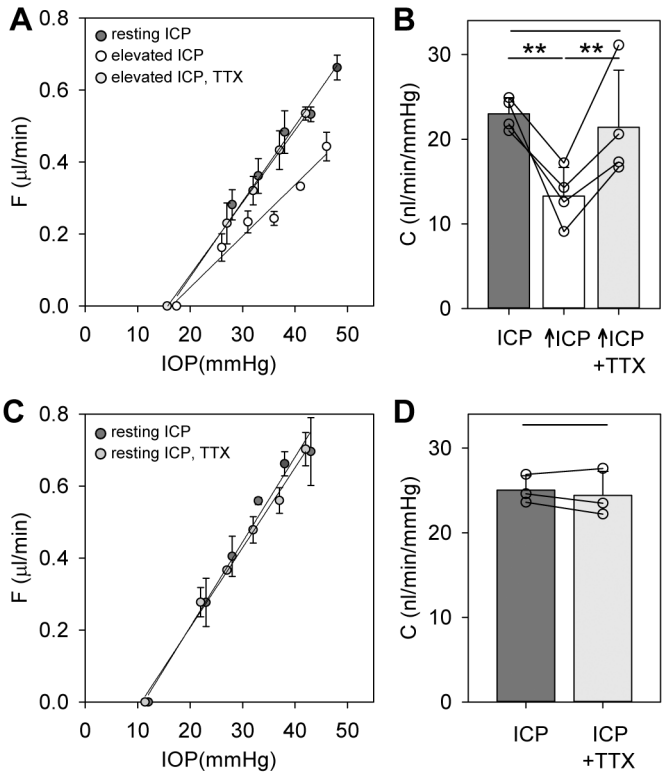

Figure 5.

TTX blocks the ICP effect. A, Pressure-flow data of a rat eye at resting ICP (black symbols), 15 mmHg above resting ICP (white symbols), and 15 mmHg above resting ICP after corneal application of TTX (gray symbols). Data regression fits (lines) estimate *C* of 20 [18-22], 12 [10-14], and 20 [16-24] nl/min/mmHg, respectively. B, Average *C* for the subset of animals to which TTX was applied at elevated ICP (n = 4). C, Pressure-flow data of a rat eye at resting ICP before (black symbols) and after (gray symbols) corneal application of TTX. Data regression fits (lines) estimate *C* of 24 [21-27], and 22 [21-24] nl/min/mmHg, respectively. D, Average *C* for a group of animals to which TTX was applied at resting ICP (n = 3). Error bars give standard deviations, and asterisks indicate statistically significant differences ($p < 0.01$).

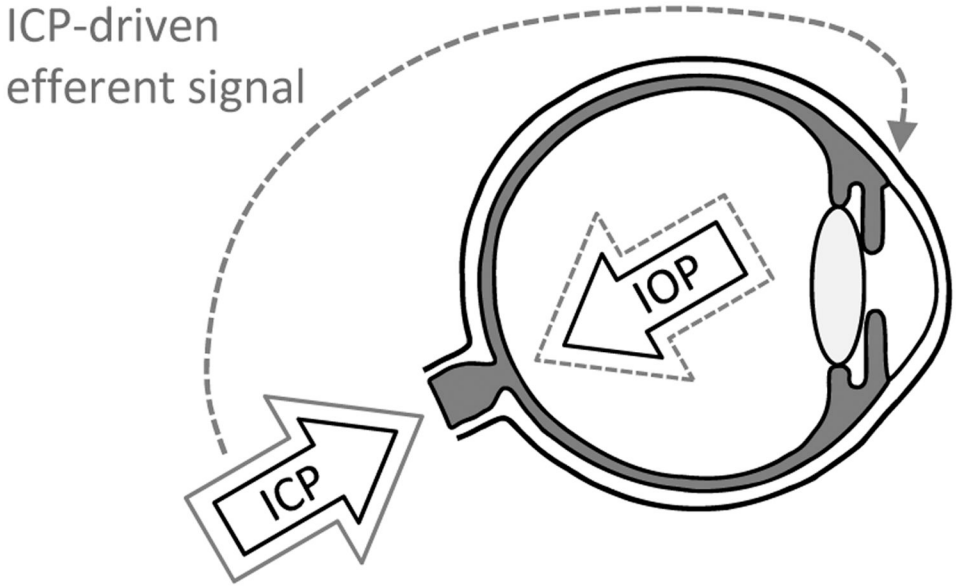

Figure 6.

Efferent feedback model of IOP modulation. Resting IOP and ICP produce baseline TLP gradient (solid black arrows). An increase in ICP (solid gray arrow) disturbs the resting TLP gradient, which poses a risk for optic nerve damage. The ICP elevation drives a neural feedback pathway that decreases the conventional outflow facility of the eye. The reduced outflow facility causes IOP to increase (dashed gray arrow), returning TLP gradient towards normal. It should be noted that the biomechanical impact of IOP and ICP changes is more spatially complex than the pointed arrows indicate, so full restoration of baseline TLP might not be necessary for protective effects.

Table 1.

ICP effects on rat aqueous humor dynamics (n = 18)

	Resting ICP	Elevated ICP
IOP (mmHg)	14.5 ± 2.0	17.5 ± 2.8 **
C (nl/min/mmHg)	22 ± 4	13 ± 3 **

** significantly different from resting value ($p < 0.01$)